

## X-Ray Diffraction Study of Macroscopic Residual Stresses of Al<sub>2</sub>O<sub>3</sub> + TiC Oxide Cutting Ceramics after Surface Machining

NĚMEČEK Jakub<sup>1,a</sup>, KOLAŘÍK Kamil<sup>1,b</sup>, ČAPEK Jiří<sup>1,c</sup>, GANEV Nikolaj<sup>1,d</sup>,  
TROJAN Karel<sup>1,e</sup> and KUZIN Valery V.<sup>2,f</sup>

<sup>1</sup>Department of Solid State Engineering, Faculty of Nuclear Science and Physical Engineering, Czech Technical University in Prague, Czech Republic

<sup>2</sup>Moscow State Technological University Stankin, Vladkovsky per. 3a, Moscow, Russia

<sup>a</sup>nemecj17@fjfi.cvut.cz, <sup>b</sup>kamil.kolarik@fjfi.cvut.cz, <sup>c</sup>jiri.capek@fjfi.cvut.cz,

<sup>d</sup>nikolaj.ganev@fjfi.cvut.cz, <sup>e</sup>karel.trojan@fjfi.cvut.cz, <sup>f</sup>dr.kuzinvalery@yandex.ru

**Keywords:** oxide cutting ceramic, X-ray diffraction, residual stresses, machining technology.

**Abstract.** Currently, the extensive research in the field of oxide cutting ceramics is conducted and there are efforts to replacement cemented carbides by these materials. The reason is better availability of the source materials and lower production costs. In cooperation with the Moscow State Technological University Stankin that provides manufacturing technology, the influence of machining technologies on the value of macroscopic residual stresses in samples of Al<sub>2</sub>O<sub>3</sub> + TiC oxide cutting ceramics were investigated by X-ray diffraction. Measurement was done for the both phases, the influence of the parameters of machining technology to residual stresses was studied and the resulting values were compared with each other.

### Introduction

At the beginning of the 20th century, the extensive research in ceramic materials began. The first material used as ceramics as a cutting tool was Al<sub>2</sub>O<sub>3</sub>. Over the years, its development had moved to a level at which it was possible to replace, for example, sintered carbides using those ceramic materials. This effort has been caused by the mechanical properties of aluminium oxide and the easy availability of the starting materials.

The starting materials and their properties have been known for a long time. The problem was to make compact replaceable cutting tool with the desired mechanical properties and dimensions. The current production process consists of three parts: first, grinding the starting material to a powder with grain size of the order of 100 nm, second, sintering the powders into a compact form and third, the surface treatment of the cutting tool to the desired dimensions.

An important technological aspect of the properties of cutting ceramics is the grain size of the starting powders. If the individual grain size is approximately the same (if they have ideal spherical shape), the uniform distribution and the pore size will be gained more easily during forming and thereby for uniform compaction throughout the volume and easier reorganization of the particles during sintering. Preference is also to achieve as small as possible grain size of the sample, because it leads to faster transport of material [1, 2].

The sintering process is very similar to that used with sintered carbides (see Fig. 1). The powder is pressed below the melting point into a compact body. But the absence of a binder which during sintering formed a liquid phase is the main difference, because it would cause degradation of mechanical properties. Today, ceramic is most commonly sintered into rods of

cross section and then cut to the desired dimensions. Individual plates are then variously surface treated and shaped [2].



Fig. 39 Scheme of creation technology of cutting ceramic sample: refinement powders (wet grinding) – evaporation – pressing – sintering

## Experiment

The influence of machining technologies on the state of residual stresses in samples of  $\text{Al}_2\text{O}_3$  with approx. 30 % of TiC oxide cutting ceramics were investigated by X-ray diffraction (XRD).

The *X'Pert PRO MPD* diffractometer was used for the samples surfaces analyses. Values of residual stresses were determined in two orthogonal directions: L (grinding/feed direction) and T (transverse direction). For  $\text{Al}_2\text{O}_3$  phase, the planes  $\{0210\}$  were analysed using manganese radiation ( $2\theta = 109^\circ$ ), and for TiC phase, the planes  $\{311\}$  were analysed using chromium radiation ( $2\theta = 123^\circ$ ).

X-ray elastic constant for the  $\text{Al}_2\text{O}_3$  phase were  $\frac{1}{2}s_2 = 3.18 \text{ TPa}^{-1}$ ,  $s_1 = -0.61 \text{ TPa}^{-1}$  and for TiC  $\frac{1}{2}s_2 = 2.63 \text{ TPa}^{-1}$ ,  $s_1 = -0.42 \text{ TPa}^{-1}$ .

## Result and discussion

**Grinding by a diamond disc.** After sintering, all samples were ground using a diamond wheel. An effect of the size of transverse displacement at constant cutting speed  $v_c = 30 \text{ m/s}$ , feed rate of the workpiece in the cutting direction  $f = 12 \text{ m/min}$  and depth of cut  $a_p = 0.04 \text{ mm}$  was observed. Values of transverse displacement is given in Tab. 1.

Tab. 7 Parameters of grinding by diamond disc

Sample	Transverse displacement [mm/displ.]
1	0.5
2	1.0
3	1.5

Due to the different crystallographic structure, the values of compressive residual stresses are assumed to be higher for the titanium carbide phase than for the corundum phase. This is due to the different values of the modulus of elasticity and the different slip systems for the trigonal structure of  $\text{Al}_2\text{O}_3$  and the fcc structure of TiC. This assertion was experimentally demonstrated and the resulting residual stress values are shown in Tab. 2.

Tab. 8 The values of normal  $\sigma_N$  and shear  $\sigma_S$  residual stresses after grinding by diamond disc

Al <sub>2</sub> O <sub>3</sub>		TiC	
L direction		L direction	
Sample	$\sigma_N$ [MPa]	Sample	$\sigma_N$ [MPa]
1	-216	1	-518
2	-182	2	-536
3	-165	3	-530
T direction		T direction	
Sample	$\sigma_N$ [MPa]	Sample	$\sigma_N$ [MPa]
1	-436	1	-776
2	-470	2	-805
3	-580	3	-938

It is also apparent that the stress values differ in the given directions. During machining, the grinding wheel moved in the direction L. Lower compressive residual stresses were analysed in the direction L. This effect is caused by moving the tool in the L-direction, due to the mechanical interaction of the cutting tool with the material, the so-called stretching of the subsurface layers occurs. In the T-direction, a higher displacement causes the higher compressive residual stresses for both phases. In the direction L, the higher displacement leads to the higher tensile stresses for the Al<sub>2</sub>O<sub>3</sub> phase but not for TiC. This is due to the already mentioned different slip systems of materials, generally different mechanical properties [4].

**Thermal annealing the samples after grinding by diamond disc.** Next samples were after grinding thermally annealed same time at 800°C. It is evident from Tab. 3 that the values of the residual stresses decreased considerably (mainly in direction T). In contrast, the value of microstrains and grain size given by the parameter FWHM remained almost unchanged (see [5]).

Tab. 9 The values of residual stresses after thermal annealing

Al <sub>2</sub> O <sub>3</sub>			TiC		
L direction			L direction		
Sample	$\sigma_N$ [MPa]	FWHM [° 2 $\theta$ ]	Sample	$\sigma_N$ [MPa]	FWHM [° 2 $\theta$ ]
12	-185	0.666	12	-516	0.965
13	-203	0.888	13	-290	0.609
14	-199	0.889	14	-289	0.847
T direction			T direction		
Sample	$\sigma_N$ [MPa]	FWHM [° 2 $\theta$ ]	Sample	$\sigma_N$ [MPa]	FWHM [° 2 $\theta$ ]
12	-303	0.781	12	-599	0.782
13	-359	0.802	13	-474	0.613
14	-342	0.769	14	-473	0.908

**Machining by blasting with compressed air (air abrasive machining).** In this method of machining, air of high pressure with added microparticles (size approx. 100 nm) is jetted on a rotating sample (see Fig. 2). The effect of air pressure changes on the residual stress in the sample was studied (see Tab. 4) with constant time of blasting  $T = 60$  s and rotate per minute  $RPM = 50$ .

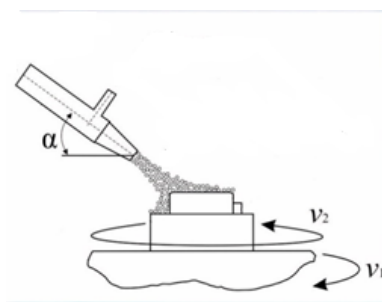


Fig. 40 Scheme of air abrasive machining

Tab. 10 Parameters of air abrasive machining

Sample	Air pressure [bar]
4	1.5
5	2.0
6	2.5

The obtained values of residual stresses (Tab. 5) show that when a pressure increases from 2 to 2.5 bars a decrease of compressive residual stresses (stress relaxation) is observed. It is probably a result of overcoming the yield strength of the material. Perhaps machining process with higher pressure values influences deeper sub-surface layers of material. The energy required for crack propagation is therefore higher for these seemingly lower compressive residual stresses. To confirm this assertion, a depth-profile analysis of residual stresses by sequential force-free etching of surface layers is needed.

Rotational movement of the specimens during the machining leads to an isotropic stress distribution i.e., the values in both the directions L and T are similar.

Tab. 11 Values of residual stresses after air abrasive machining

Al <sub>2</sub> O <sub>3</sub>		TiC	
L direction		L direction	
Sample	$\sigma_N$ [MPa]	Sample	$\sigma_N$ [MPa]
4	-352	4	-799
5	-367	5	-928
6	-242	6	-278
T direction		T direction	
Sample	$\sigma_N$ [MPa]	Sample	$\sigma_N$ [MPa]
4	-295	4	-737
5	-389	5	-899
6	-284	6	-283

**Water Jet Machining (WJM).** This technology is based on the same principle as air abrasive machining, when a focused beam of water is jetted out by varying the pressure on the rotating sample for 60 seconds (see Fig. 3 and Tab. 6)

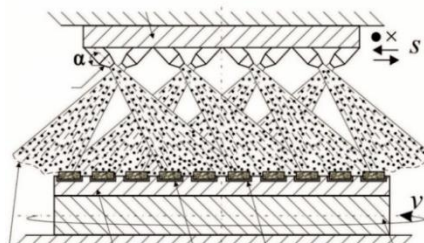


Fig. 41 Scheme of WJM

Tab. 12 Parameters of WJM

Sample	Water pressure [bar]
7	1.5
8	2.0
9	2.5

It is evident, that the yield strength value has not been overcome for applied values of pressure jetting, see Tab. 7. The values of residual compressive residual stresses increase steadily with increasing pressure in contrast to the samples after air abrasive machining. Due to the rotating of the samples an isotropic residual stress distribution is achieved again.

Tab. 13 Values of residual stresses for WJM

Al <sub>2</sub> O <sub>3</sub>		TiC	
L direction		L direction	
Sample	$\sigma_N$ [MPa]	Sample	$\sigma_N$ [MPa]
7	-99	7	-406
8	-149	8	-363
9	-255	9	-568
T direction		T direction	
Sample	$\sigma_N$ [MPa]	Sample	$\sigma_N$ [MPa]
7	-85	7	-374
8	-166	8	-364
9	-238	9	-484

**Laser Shock Peening.** By this technology the effect of power changes of pulse laser on surface residual stresses was studied (see Tab. 8). The displacement of the laser at each spot is larger than the radius of the spot. The constant parameters of machining were the frequency of laser  $f = 30$  Hz and displacement at one pulse  $s_x = s_y = 30$   $\mu\text{m}$ , see Fig. 4.

Laser machining leads to sample heating and a subsequent decrease in residual stresses, which in this case will mainly be transformation stresses. Increasing power will result in higher temperatures and thus greater so-called stress relaxation, which correlates with a different phase representation. In addition, the influence of overlapping on the anisotropy of residual stresses distribution can be observed (see Tab. 9).

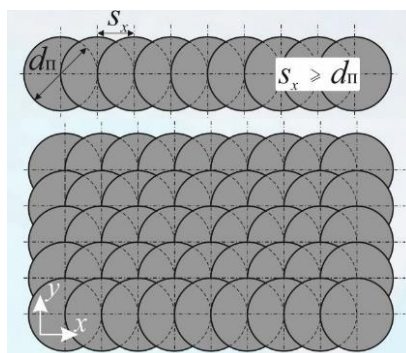


Fig. 42 Scheme of linear and surface laying of spots

Tab. 14 Variable parameter of Laser Shock Peening

Sample	Power [W]
10.1	2
10.2	5
10.3	10
10.4	15

Tab. 15 Values of residual stresses after Laser Shock Peening

Al <sub>2</sub> O <sub>3</sub>		TiC	
L direction		L direction	
Sample	$\sigma_N$ [MPa]	Sample	$\sigma_N$ [MPa]
10.1	-53	10.1	-318
10.2	31	10.2	-259
10.3	-29	10.3	-200
10.4	-62	10.4	-220
T direction		direction	
Sample	$\sigma_N$ [MPa]	Sample	$\sigma_N$ [MPa]
10.1	-155	10.1	-509
10.2	-125	10.2	-448
10.3	-71	10.3	-367
10.4	-48	10.4	-288

**Friction tests.** After grinding of samples by diamond disc their surface was loaded by rotating steel disk at different time intervals, see Tab. 10. The influence of time of friction on values of residual stresses was investigated.

Tab. 16 Parameters of friction tests

Sample	Time of loading [s]
11.1	2
11.2	6
11.3	12

Due to friction, the surface of the sample was plastically deformed and heated, which could cause thermal stress relaxation. Another possibility is that the surface could crack. Tab. 11 shows that TiC is more sensitive to loading than Al<sub>2</sub>O<sub>3</sub>, as changes in residual stress values for titan carbide are greater than for alumina. This can also be explained by the different structure of these phases and different thermo-mechanical properties, e.g. slip systems.

Tab. 17 Values of residual stresses after friction test

Al <sub>2</sub> O <sub>3</sub>		TiC	
L direction		L direction	
Sample	$\sigma_N$ [MPa]	Sample	$\sigma_N$ [MPa]
11.1	-42	11.1	-453
11.2	3	11.2	-129
11.3	-78	11.3	-242
T direction		T direction	
Sample	$\sigma_N$ [MPa]	Sample	$\sigma_N$ [MPa]
11.1	-145	11.1	-348
11.2	-15	11.2	-190
11.3	47	11.3	-240

## Conclusions

Values of residual stresses of cutting ceramics Al<sub>2</sub>O<sub>3</sub> + TiC were analysed in two perpendicular directions. The influence of machining technologies to residual stresses was studied in the both phases.

Anisotropy and different values of residual stresses for both the phases during grinding by diamond disc were obtained, and the thermal relaxation of macroscopic residual stresses after thermal annealing was also analysed.

For air abrasive cutting overcoming of the yield stress was found out with increasing the pressure to 2.5 MPa. Due to rotational movement during air abrasive machining and water jet machining the values of surface residual stresses are isotropic.

Samples machined by laser exhibit thermal relaxation of residual stresses. At the same time, the observed anisotropy of state of residual stresses is due to overlapping of laser-processed areas.

On the samples after the loading tests thermal relaxation of residual stresses was observed. It was shown that titan carbide is more sensitive to load than alumina.

## Acknowledgement

This work was supported by the Grant Agency of the Czech Technical University in Prague, grant No. SGS16/245/OHK4/3T/14.

## References

- [1] A. Humár, Materiály pro řezné nástroje. MM publishing, Prague, 2008.
- [2] C. B. Carter, M. G. Norton, Ceramic materials: science and engineering. Second edition, Springer Science & Business Media, New York, 2013.
- [3] V. Kuzin, N. R. Portnoi, S. Yu. Fedorov, V. I. Moroz, Effect of Air-Abrasive Treatment on Oxide-Carbide Ceramic Object Operating Properties. Refractories & Industrial Ceramics, 2016, 56.5.
- [4] P. Putyra, S. Skrzypek, B. Smuk, M. Posiadło, Analysis of residual stresses using the  $\sin^2\psi$  method for Al<sub>2</sub>O<sub>3</sub> materials before and after grinding and heat treatment processes. Materiały Ceramiczne, 2010, 62.3, 301-306 s.
- [5] J. Němeček, Diffraction study of selected characteristic of cutting ceramics, Praha, 2017, Diploma thesis, CTU in Prague, Faculty of Nuclear Science and Physical Engineering, 2017-6-15